Research Article | Vol. 26, No. 4 | 19 Feb 2018 | OPTICS EXPRESS 5083
Optics EXPRESS

Nonlinear frequency up-conversion via double topological edge modes

CHENG QIAN,[1] KA HEI CHOI,[1] RAYMOND P. H. WU,[1] YONGLIANG ZHANG,[1] KAI GUO,[1,2] AND KIN HUNG FUNG[1,*]

[1]*Department of Applied Physics, The Hong Kong Polytechnic University, Hong Kong, China*
[2]*School of Computer and Information, Heifei University of Technology, Hefei, 230009, China*
[*]*khfung@polyu.edu.hk*

Abstract: We study the nonlinear frequency up-conversion in a plasmonic thin film sandwiched between one-dimensional photonic crystals (PCs) of different Zak phases by rigorous numerical time-domain nonlinear hydrodynamic calculations. We show that the proposed hetero-structure can support robust fundamental and high-order topological edge modes that simultaneously enhance the third-harmonic generation. Numerical simulations also show that femtosecond pulses can excite double topological edge modes through optical tunneling in band gaps, leading to a large nonlinear response. The obtained third harmonic generation (THG) conversion efficiency of the hetero-structure is three orders of magnitude larger than that of a single plasmonic film. The results presented here may open new avenues for designing high-efficiency nonlinear photonic devices.

OCIS codes: (190.2620) Harmonic generation and mixing; (230.5298) Photonic crystals; (350.1370) Berry's phase.

References and links

1. M. Kauranen and A. V. Zayats, "Nonlinear plasmonics," Nat. Photonics **6**(11), 737–748 (2012).
2. I.-Y. Park, S. Kim, J. Choi, D.-H. Lee, Y.-J. Kim, M. F. Kling, M. I. Stockman, and S.-W. Kim, "Plasmonic generation of ultrashort extreme-ultraviolet light pulses," Nat. Photonics **5**(11), 677–681 (2011).
3. J. Butet, P.-F. Brevet, and O. J. Martin, "Optical second harmonic generation in plasmonic nanostructures: from fundamental principles to advanced applications," ACS Nano **9**(11), 10545–10562 (2015).
4. S. Chen, G. Li, F. Zeuner, W. H. Wong, E. Y. B. Pun, T. Zentgraf, K. W. Cheah, and S. Zhang, "Symmetry-selective third-harmonic generation from plasmonic metacrystals," Phys. Rev. Lett. **113**(3), 033901 (2014).
5. O. Gazzano, S. Michaelis de Vasconcellos, K. Gauthron, C. Symonds, J. Bloch, P. Voisin, J. Bellessa, A. Lemaître, and P. Senellart, "Evidence for Confined Tamm Plasmon Modes under Metallic Microdisks and Application to the Control of Spontaneous Optical Emission," Phys. Rev. Lett. **107**(24), 247402 (2011).
6. T. Goto, A. V. Dorofeenko, A. M. Merzlikin, A. V. Baryshev, A. P. Vinogradov, M. Inoue, A. A. Lisyansky, and A. B. Granovsky, "Optical Tamm states in one-dimensional magnetophotonic structures," Phys. Rev. Lett. **101**(11), 113902 (2008).
7. I. Iorsh, I. V. Shadrivov, P. A. Belov, and Y. S. Kivshar, "Nonlinear Tamm states in layered metal–dielectric metamaterials," Phys. Status Solidi **6**(1), 43–45 (2012).
8. B. I. Afinogenov, V. O. Bessonov, and A. A. Fedyanin, "Second-harmonic generation enhancement in the presence of Tamm plasmon-polaritons," Opt. Lett. **39**(24), 6895–6898 (2014).
9. Z. Hai-Chun, Y. Guang, W. Kai, L. Hua, and L. Pei-Xiang, "Coupled Optical Tamm States in a Planar Dielectric Mirror Structure Containing a Thin Metal Film," Chin. Phys. Lett. **29**(6), 067101 (2012).
10. K. J. Lee, J. W. Wu, and K. Kim, "Enhanced nonlinear optical effects due to the excitation of optical Tamm plasmon polaritons in one-dimensional photonic crystal structures," Opt. Express **21**(23), 28817–28823 (2013).
11. K. Leosson, S. Shayestehaminzadeh, T. K. Tryggvason, A. Kossoy, B. Agnarsson, F. Magnus, S. Olafsson, J. T. Gudmundsson, E. B. Magnusson, and I. A. Shelykh, "Comparing resonant photon tunneling via cavity modes and Tamm plasmon polariton modes in metal-coated Bragg mirrors," Opt. Lett. **37**(19), 4026–4028 (2012).
12. H. Zhou, G. Yang, K. Wang, H. Long, and P. Lu, "Multiple optical Tamm states at a metal-dielectric mirror interface," Opt. Lett. **35**(24), 4112–4114 (2010).
13. N. Horiuchi, "Topological insulators: Nonlinear opportunities," Nat. Photonics **9**(12), 784 (2015).
14. L. Lu, J. D. Joannopoulos, and M. Soljačić, "Topological states in photonic systems," Nat. Phys. **12**(7), 626–629 (2016).
15. L. Lu, J. D. Joannopoulos, and M. Soljačić, "Topological photonics," Nat. Photonics **8**(11), 821–829 (2014).
16. M. Soljacić and J. D. Joannopoulos, "Enhancement of nonlinear effects using photonic crystals," Nat. Mater. **3**(4), 211–219 (2004).
17. W. P. Su, J. R. Schrieffer, and A. J. Heeger, "Solitons in Polyacetylene," Phys. Rev. Lett. **42**(25), 1698–1701 (1979).

#312350 https://doi.org/10.1364/OE.26.005083
Journal © 2018 Received 31 Oct 2017; revised 23 Dec 2017; accepted 22 Jan 2018; published 16 Feb 2018

Optics EXPRESS

18. M. Xiao, Z. Zhang, and C. T. Chan, "Surface impedance and bulk band geometric phases in one-dimensional systems," Phys. Rev. X **4**(2), 021017 (2014).
19. Q. Wang, M. Xiao, H. Liu, S. Zhu, and C. Chan, "Measurement of the Zak phase of photonic bands through the interface states of a metasurface/photonic crystal," Phys. Rev. B **93**(4), 041415 (2016).
20. K. H. Choi, C. W. Ling, K. F. Lee, Y. H. Tsang, and K. H. Fung, "Simultaneous multi-frequency topological edge modes between one-dimensional photonic crystals," Opt. Lett. **41**(7), 1644–1647 (2016).
21. A. V. Krasavin, P. Ginzburg, G. A. Wurtz, and A. V. Zayats, "Nonlocality-driven supercontinuum white light generation in plasmonic nanostructures," Nat. Commun. **7**, 11497 (2016).
22. J. Benedicto, R. Pollès, C. Ciracì, E. Centeno, D. R. Smith, and A. Moreau, "Numerical tool to take nonlocal effects into account in metallo-dielectric multilayers," J. Opt. Soc. Am. A **32**(8), 1581–1588 (2015).
23. C. Ciracì, E. Poutrina, M. Scalora, and D. R. Smith, "Second-harmonic generation in metallic nanoparticles: Clarification of the role of the surface," Phys. Rev. B **86**(11), 115451 (2012).
24. C. Ciracì, E. Poutrina, M. Scalora, and D. R. Smith, "Origin of second-harmonic generation enhancement in optical split-ring resonators," Phys. Rev. B **85**(20), 201403 (2012).
25. M. Fang, Z. Huang, W. E. Sha, X. Y. Xiong, and X. Wu, "Full Hydrodynamic Model of Nonlinear Electromagnetic Response in Metallic Metamaterials," arXiv preprint arXiv:1610.09624 (2016).
26. Y. Zhao and J. Liu, "FDTD for Hydrodynamic Electron Fluid Maxwell Equations," Photonics **2**(2), 459–467 (2015).
27. A. Hille, M. Moeferdt, C. Wolff, C. Matyssek, R. Rodríguez-Oliveros, C. Prohm, J. Niegemann, S. Grafström, L. M. Eng, and K. Busch, "Second harmonic generation from metal nano-particle resonators: Numerical analysis on the basis of the hydrodynamic drude model," J. Phys. Chem. C **120**(2), 1163–1169 (2016).
28. S. Ghosh, N. Chakrabarti, and F. Haas, "New nonlinear structures in a degenerate one-dimensional electron gas," Europhys. Lett. **105**(3), 30006 (2014).

1. Introduction

Over the past decades, nonlinear optical effects aroused extensive research activities [1–4]. Unfortunately, as optical nonlinearities are inherently weak, there is a pressing need to find efficient physical mechanisms that could improve the ability to increase the effective nonlinear optical response and design high-efficiency nonlinear optical devices. Photonic surface modes that has been theoretically or experimentally demonstrated in the photonic crystal structures have drawn more and more attention. With the help of plasmonic effects excited at the interface [5–9], an increased effective nonlinear optical response could be achieved [10–12]. There are good reasons to use multilayer structures for enhancing the nonlinear effects. On one hand, plasmonic excitations bring up strong electromagnetic field localization enhancing nonlinear optical process. On the other hand, multilayer structures containing a plasmonic film are easy to fabricate.

It would be even more interesting if the multilayer structures can be used to support topological robustness for nonlinear optics. Topological photonics, originally developed from condensed matter theory, has led to many new discoveries and potential applications [13–16]. In 1-D periodic systems, the SSH model was firstly discovered by Su, Schrieffer and Heeger to explain the existence of edge modes in polyacetylene [17]. Recently, Zak phase and topological surface modes, in 1-D photonic crystals were theoretically investigated and experimentally measured [18,19]. Furthermore, it has been shown that 1D binary PC can be designed in a way such that topological edge modes can be supported in any photonic bandgaps [20]. Based on our previous work, a topological approach is applied to guarantee simultaneous creation of robust topological edge modes and enhancement of the light-matter interaction at both excitation and emission frequencies of frequency conversion processes.

In this work, we have performed the first attempt to use a pair of topological edge modes at different frequencies to enhance nonlinear frequency conversion in a thin plasmonic film.

2. Nonlinear plasmonic structure and time-domain simulation

We consider a nonlinear thin plasmonic film sandwiched between two binary PCs. As shown in Fig. 1(a), the thickness of the plasmonic thin film d_M is set to be $5\,\mathrm{nm}$, that is slightly larger than the skin depth of plasmonic film and thin enough to contribute less influence on the transmission spectrum compared with the PC structure depicted in Fig. 1(b). A detailed structure is given as follows. $\varepsilon_A = 6.3$, $\varepsilon_B = 2.25$, $\varepsilon_C = 7.13$, $\mu_A = \mu_B = \mu_C = 1$. The period

Optics EXPRESS

$\Lambda = 1000\text{nm}$ of a unit cell is determined by $\Lambda = d_A + d_B$, and the thickness of the dielectric layer A, B, and C is shown in Fig. 1, $d_A = 0.396\Lambda$, $d_B = 0.604\Lambda$ in PC X and $d_C = 0.342\Lambda$, $d_B = 0.658\Lambda$ in PC Y'. It is a fairly complicated task to describe the inherent nonlinear responses of the plasmonic film. Along with phenomenological models, based on experimental retrieval of nonlinear susceptibilities, a hydrodynamic model, treating the electron plasma by means of a charged fluid, is shown to give a qualitative description of the nonlinear interaction [21–28].The mesoscopic hydrodynamic model has been applied to simulate the nonlinear response of the hetero-structure and to provide a full picture of the nonlinear physical process.

Here, we briefly describe our model and algorithm. We use a set of self-consistent hydrodynamic Eqs. (1)-(4) to describe the interaction between the electromagnetic fields (E and H) and electron gas in the plasmonic films as [25],

$$\nabla \times \mathbf{E} = -\mu \frac{\partial \mathbf{H}}{\partial t}, \tag{1}$$

$$\nabla \times \mathbf{H} = ne\mathbf{u} + \varepsilon \frac{\partial \mathbf{E}}{\partial t}, \tag{2}$$

$$\frac{\partial n}{\partial t} + \nabla \cdot (n\mathbf{u}) = 0, \tag{3}$$

$$mn\left[\frac{\partial \mathbf{u}}{\partial t} + (\mathbf{u} \cdot \nabla)\mathbf{u} + \gamma \mathbf{u}\right] = en\mathbf{E} + en\mu \mathbf{u} \times \mathbf{H} - \nabla p, \tag{4}$$

where ε and μ are the permittivity and permeability, respectively, e and m are the electron charge and electron effective mass respectively. In the region where only dielectric is considered, the free electron density n will be set to zero, and ε and μ become the permittivity and permeability of the media. In Eq. (4), γ denotes the damping rate and the Fermi pressure p is given by [27],

$$p = \frac{\hbar^2 \left(3\pi^2\right)^{\frac{2}{3}}}{5m} (n)^{\frac{5}{3}}, \tag{5}$$

Equations (1) and (2) are the macroscopic Maxwell's equations while Eqs. (3) and (4) are the electron fluid equations that represents the dynamics of electrons in a plasmonic system, representing conservation of mass and momentum. n is the electron number density and $\mathbf{u}$ is the mean electron velocity.

In Eq. (2) the term $ne\mathbf{u}$ represents the current density and is the bridge between Maxwell's equations and electron fluid equations. The convection term $(\mathbf{u} \cdot \nabla)\mathbf{u}$, magnetic term $\mathbf{u} \times \mathbf{H}$ and quantum effect term ∇p will contribute to the nonlocal and nonlinear effects. Equations (1)-(5) constitute a self-consistent electromagnetic-hydrodynamic model that can describe the behaviour of electron gas considering both nonlocal and nonlinear effects in plasmonic systems.

Optics EXPRESS

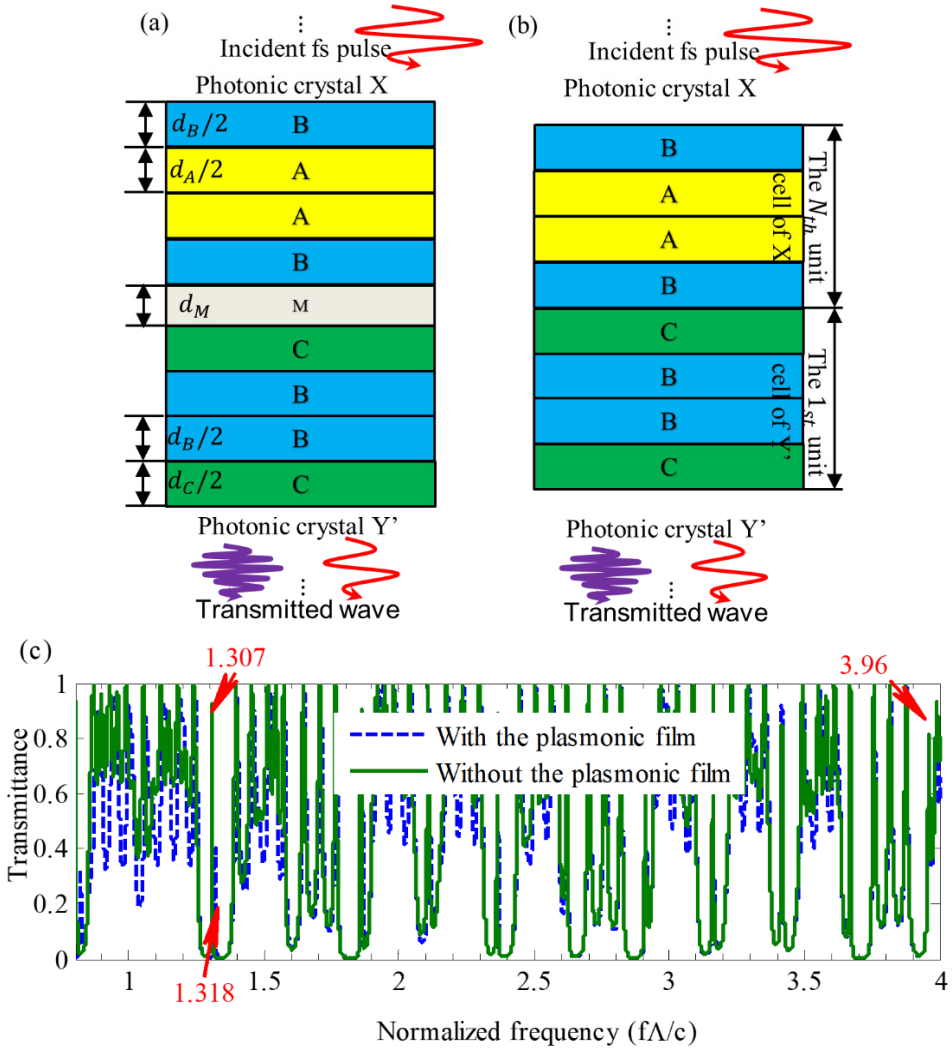

Fig. 1. (a), (b) Schematic view of the 1-D binary PCs model constructed by connecting two 1-D PCs X and Y' with (a) and without (b) a thin plasmonic film at the centre, where X and Y' contain N unit cells with the period $\Lambda = 1000\text{nm}$. The parameters of PC X are given by $d_A = 0.396\Lambda$, $n_A = 2.51$, $d_B = 0.604\Lambda \cdot n_B = 1.5$, $\mu_A = \mu_B = 1$ and the parameters of PC Y' are given by $d_C = 0.342\Lambda$, $n_C = 2.67$, $d_B = 0.658\Lambda$, $n_B = 1.5$, $\mu_c = \mu_B = 1$. The thickness of the plasmonic film $d_M = 5\text{nm}$. (c) Transmission spectrum of the 1-D binary PC with (blue dashed line) and without (green solid line) a $5nm$ plasmonic film, when the number of unit cells $N = 4$ on both sides.

In the simulation, the initial electric density and damping rate is set to be $n_0 = 3.5\times10^{28}\,\text{m}^{-3}$ and $\gamma = 4.6\times10^{13}\,\text{s}^{-1}$ respectively. The effective mass $m = 0.65m_e$, where m_e is the free electron mass [23-24]. In order to confine the electron fluid to the nano-film, the so-called slip boundary condition is applied that the normal component of the current density vanishes at the plasmonic film's surface $\mathbf{n}\cdot\mathbf{u} = 0$, while electron motion tangential to the plasmonic film's surface is allowed. Mur absorbing boundary condition is used along the propagating direction as shown in Fig. 1(a).

Optics EXPRESS

The FDTD method [25,26] is applied to solve the above set of self-consistent partial differential equations (PDEs) (1)-(5) in space and time. The numerical scheme can be summarized as follows,

In our FDTD simulation, we discretize Eqs. (1)-(5) with the standard grid, leapfrog in time approach. The incident wave is polarized in the z direction and propagates along the x-axis. The electric field components E_x, E_z, and electron density n are at the integer-grids. The magnetic component H_y, mean electron velocity components u_x, and u_z are at the half-grids in the FDTD scheme. After employing the central difference scheme for the time stepping, the set of PDEs can be made into a set of algebraic equations. Using the initial electron density and damping rate, all the unknowns can be calculated at each time step. Explicit time domain simulations that allow the visualization of electron gas fluid and dynamic variation of electromagnetic fields, will open up new understanding in these simulations. Hence, the FDTD simulation solver for the hydrodynamic model is a useful tool in the study of nonlinear topological photonic systems. The proposed time-domain model takes both linear and nonlinear dynamics of the electron gas into consideration and does not rely on the experimentally measured bulk and surface nonlinear susceptibilities. With the help of the classical time-domain FDTD approach, the hydrodynamic equations are solved nonperturbatively.

3. Band gap and edge states

The schematic of our system is illustrated in Fig. 1. Firstly, we analyse the characteristics of the $X+Y'$ PCs shown in Fig. 1(b) without a plasmonic film inserted at the centre of the interface between two PCs. The thickness of a single dielectric layer is specified by Eq. (6) as,

$$\alpha\Lambda = n_A d_A + n_B d_B, \tag{6}$$

where $\alpha = 1.9$ is the ratio of optical path length of a unit cell to its period. The period $\Lambda = 1000\text{nm}$ of a unit cell is determined by $\Lambda = d_A + d_B$, and the detailed thickness of the dielectric layer A, B, and C is shown in Fig. 1. For each photonic passband m, we define the Zak phase (i.e., the topological invariant) as [18–20],

$$\theta_m^{\text{Zak}} = \int_{-\frac{\pi}{\Lambda}}^{\frac{\pi}{\Lambda}} \left[i \int_{\text{unit cell}} \varepsilon(z) u_{m,K}^*(z) \partial_K u_{m,K}(z) dz \right] dK, \tag{7}$$

Where $i\int_{\text{unit cell}} \varepsilon(z) u_{m,K}^*(z) \partial_K u_{m,K}(z) dz$ is the berry connection, $\varepsilon(z)$ is the function of permittivity, and $u_{m,K}(z)$ is the periodic-in-cell part of the Bloch electric field eigenfunction of a state on the mth band with a Bloch wave vector K.

Figures 2(b) and 2(c) show the photonic band structure of PC X and PC Y' from the 0th gap to the 15th gap, where the Zak phase of each passband is labelled at the center of its own band. In Fig. 2(a), topological edge modes can be observed at all photonic bandgaps in the transmission spectrum of $X+Y'$ PCs calculated by the transfer matrix method. As the difference of the sums of the Zak phases $\sum_i^m \theta_i^{\text{Zak}}$, for PC X and PC Y', are 3π, except that the first bandgap has the difference of π only, it implies that topological edge modes will exist at every bandgap. Relevant discussion is detailed in [20]. Furthermore, the proposed $X+Y'$ PCs could support robust topological edge states and be applied to enhance nonlinear light-matter interactions such as second harmonic generation (SHG), third harmonic generation (THG), and four-wave mixing (FWM), and so on. It could be predicted that the simultaneous topological edge modes bring up with the significant strong electromagnetic

Optics EXPRESS

field localization at the interface for both fundamental frequency and higher harmonics. As a result, high nonlinearity conversion efficiency can be achieved.

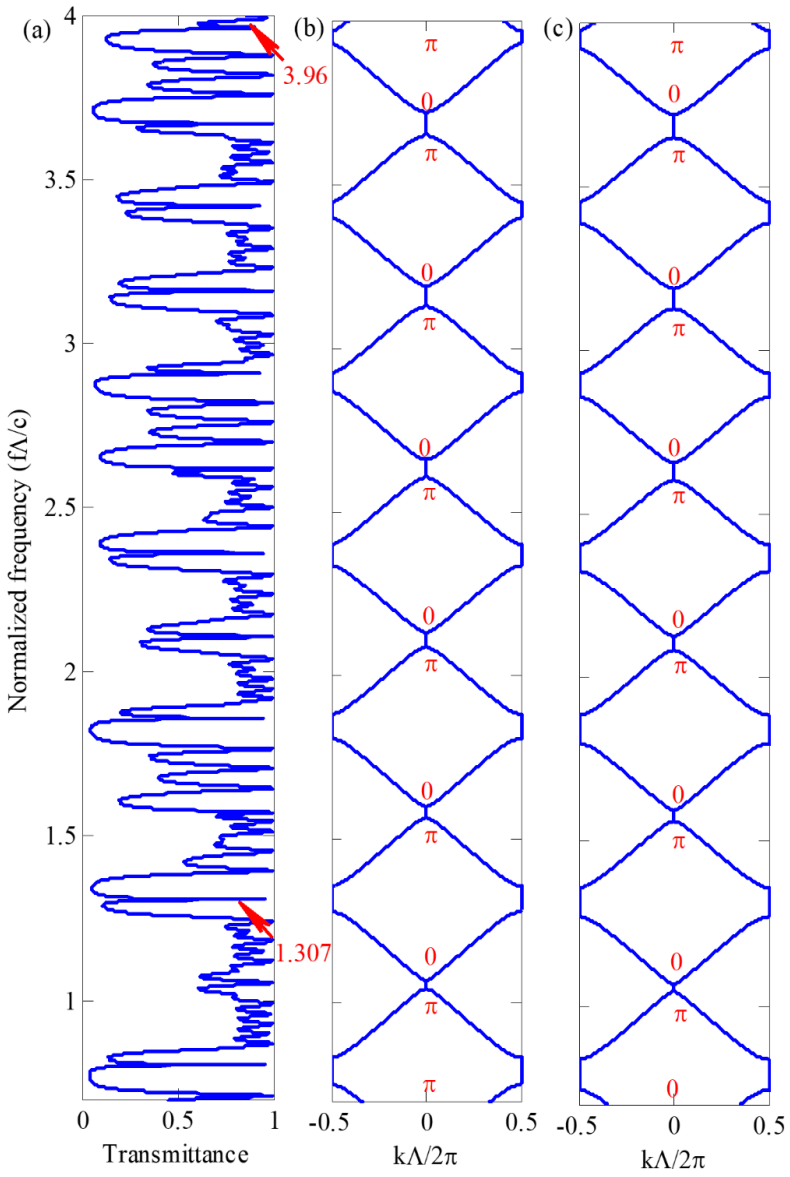

Fig. 2. (a) The transmission spectrum of $X+Y'$ PCs, where the number of unit cells $N=4$ on both sides. The parameters of PC X are given by $n_A=2.51$, $n_B=1.5$, $d_A=0.396\Lambda$, $d_B=0.604\Lambda$, and the parameters of PC Y' are given by $n_B=1.5$, $n_C=2.67$, $d_B=0.658\Lambda$, $d_C=0.342\Lambda$, where $\Lambda=1000\text{nm}$ is the unit length of the PCs. Red arrows indicate that there are fundamental and third harmonic topological edge modes. (b), (c) Real part of complex band structure (solid blue curve) of PC X and PC Y', and the Zak phase of each individual band is also labelled in (b) and (c).

Based on the $X+Y'$ PCs' structure discussed previously, we choose the parameters similar to silver, which is appealing for potential use in nonlinear optical applications at

Optics EXPRESS

visible and ultraviolet wavelength, for the thin plasmonic film at the centre of the $X+Y'$ PCs. The detailed hetero-structure is illustrated in Fig. 1(a). A TM polarized plane wave from free-space incidents normally on the 1-D binary PCs containing a plasmonic film of thickness $d_M = 5\text{nm}$. As shown in Fig. 1(c), the transmission spectrum in the linear optics regime obtained by the FDTD method, based on the (nonlinear) hydrodynamic model. It should be noted that the input amplitude for the results in Fig. 1 is far less than the nonlinear threshold of the plasmonic materials, so that the nonlinear terms in the hydrodynamic model do not take effect and the proposed the hetero-structure is equivalent to a linear system. Due to the insertion of the plasmonic film, the transmittance is reduced a little at the passbands. However, it can be observed in Fig. 1(c) that the thickness of the plasmonic film is thin enough to introduce slight influence on the 1-D binary PCs, especially at the bandgaps.

In this work, we chose the fundamental and third harmonic topological edge modes (indicated by red arrows) at the 3rd and 15th bandgap to provide the double-resonance and obtain the nonlinear enhancement. At the 3rd bandgap, for the fundamental topological edge mode, the normalized frequency is slight blue shift from 1.307 (PCs without the plasmonic film indicated by green solid line) to 1.318 (PCs with the plasmonic film indicated by blue dashed line). Meanwhile, At the 15th bandgap, for the third harmonic topological edge mode, the normalized frequency is almost the same at 3.96 , and nearly three times the normalized frequency for the fundamental topological edge mode in the hetero-structure. As a result, the double topological edge modes can be excited in the hetero-structure to guarantee effective third harmonic generation.

4. Harmonic generation and nonlinear enhancement

Here, we investigate the nonlinear response from the 1-D hetero-structure illuminated by a sine-modulated Gaussian pulse based on the numerical solver presented in the previous section. The simulation domain is the same as in Fig. 1(a) while the incident wave become a Gaussian pulse with E_z^{inc} polarized in the z direction and propagates along the x-axis. Its profile is defined by,

$$E_z^{\text{inc}} = E_0 \sin\left(2\pi f_0 t\right) \exp\left[-\frac{4\pi\left(t-t_0\right)^2}{\tau^2}\right], \tag{8}$$

where E_0 is the peak electric field and $t_0 = 3\tau$ is the temporal offset with the temporal width $\tau = 600\text{fs}$. The maximal peak intensity of $I_0 = 4.247\times10^{14}\,\text{w}/\text{m}^2$ is selected to ensure a stable and significant high order harmonic generation. The spatial and temporal step sizes are set to be $\Delta x = 1\text{nm}$ and $\Delta t = \frac{1}{3}\times10^{-17}\text{s}$ according to the Courant-Friedrichs limit (CFL) condition. The fundamental frequency $f_0 = 395.4\text{THz}$, corresponding to the normalized frequency 1.318 , so that the fundamental topological edge mode will be excited.

In Fig. 3(a), the time-dependent transmitted electric field through the hetero-structure is Fourier transformed and the third harmonic frequency component is detected. By varying the incident pump power, the power-dependent third harmonics are also plotted. It can be observed that with the help of the double topological edge modes supported by the hetero-structure, significant third harmonic generation phenomena will occur. As the increase of the incident peak electric field amplitude from $0.1E_0$ to E_0 , the detected third harmonics intensity is also increased. In Fig. 3(b), it is demonstrated that the relationship between the peak intensity of the third harmonics and the cubic power of the fundamental intensity is almost linear. It implies that higher incident pump power produce more significant third harmonics.

Optics EXPRESS

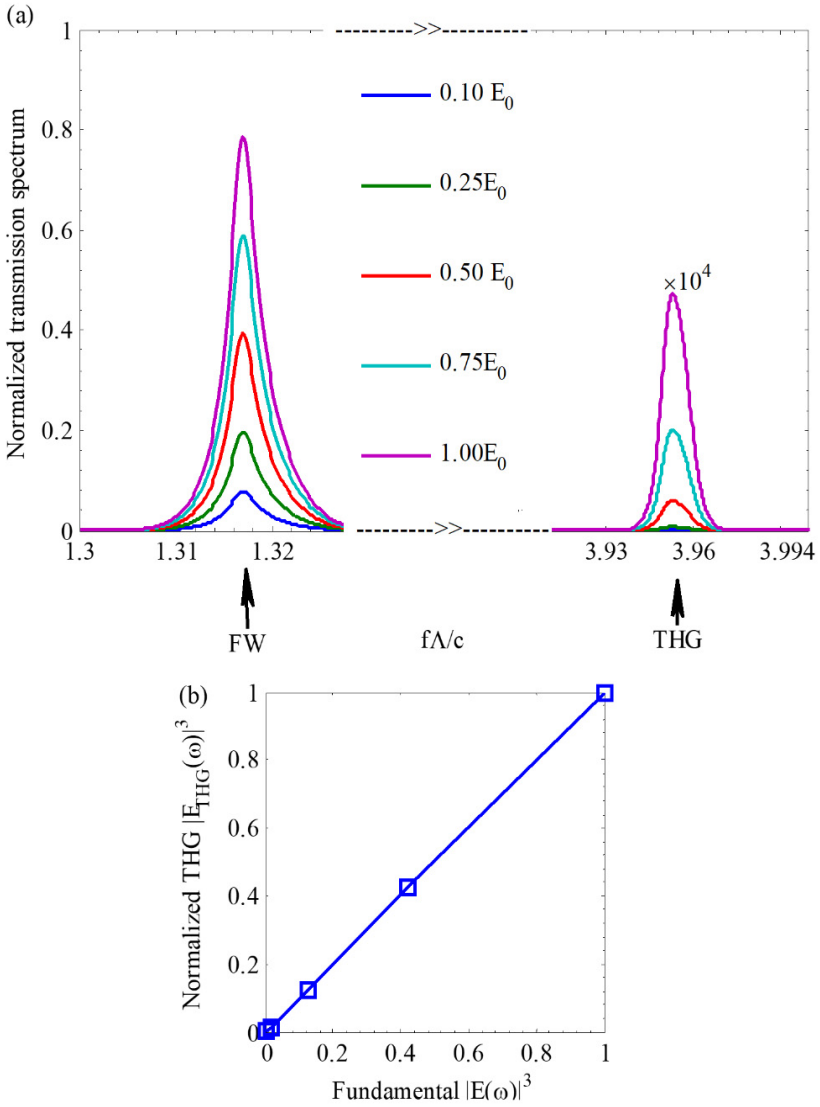

Fig. 3. (a) Nonlinear transmission spectrum for the 1-D binary PC containing a thin plasmonic film with different input pump power. (b) The peak intensities of the third harmonics vs. the third power of the fundamental intensities.

In the proposed 1-D binary PCs containing a thin plasmonic film structure, the fundamental topological edge mode creates a strong boost in the intensity field of incident far-red pulse ($f_0 = 395.4\text{THz}, \lambda_0 = 758.7\text{nm}$). Consequently, ultraviolet pulses ($f_{\text{THG}} = 1186.2\text{THz}, \lambda_0 = 253\text{nm}$) can be detected by means of high-harmonic generation through the light-matter interaction at the interface between the plasmonic film and the dielectric. In Fig. 4(a), the comparison between the hetero-structure and the single plasmonic film about the nonlinear transmission spectrum is provided. When the maximal peak intensity is I_0, even fifth-order harmonic generation can be detected in the hetero-structure. The robust double topological edge modes that supported by the hetero-structure make it a good candidate for high-order harmonic generation enhancement. In particular, we obtain

Optics EXPRESS

conversion efficiency of the hetero-structure $\eta \sim 2.23\times10^{-9}$, and the conversion efficiency is significant improved, compared with that of the single plasmonic film $\eta \sim 2.81\times10^{-12}$. In Fig. 4(b), we provide the input intensity versus the conversion efficiency. It can be concluded that taking advantage of the nonlinear enhancement via double topological edge modes, the third harmonic generation conversion efficiency can be increased by three orders of the magnitude.

5. Conclusion

We show by performing rigorous time-domain hydrodynamic calculations that a 1-D binary PCs supporting robust topological edge harmonic modes can simultaneously enhance odd-order harmonic generation at both excitation and emission frequency. By introducing a thin plasmonic film into such topological PCs, it is found that the third harmonic generation (THG) conversion efficiency becomes three orders of magnitude larger than that of the original single plasmonic film. Our study may suggest a new approach to achieve robust topological nonlinear plasmonic devices.

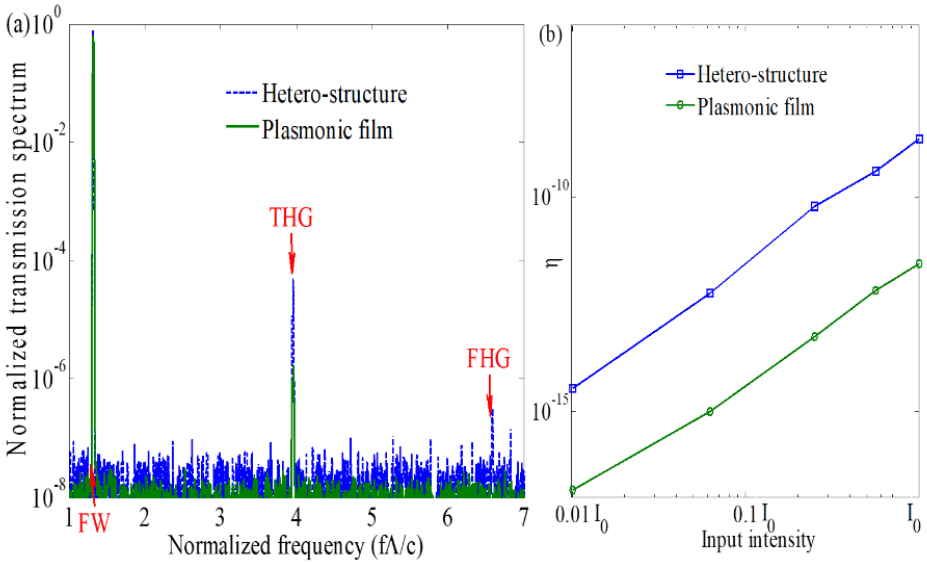

Fig. 4. (a) Nonlinear transmission spectrum for the hetero-structure 1-D binary PC containing a thin plasmonic film (blue dashed line) and a single plasmonic film (green solid line). (b) The conversion efficiency of the hetero-structure 1-D binary PC containing a thin plasmonic film (blue line with square) and a single plasmonic film (green line with circle) vs. the input intensities, when the normalized central frequency is 1.318.

Funding

Hong Kong RGC (AoE/P-02/12, 15300315); The Hong Kong Polytechnic University under grant nos. (G-UC70).